Pharmacological Research 161 (2020) 105205

Contents lists available at ScienceDirect

Pharmacological Research

journal homepage: www.elsevier.com/locate/yphrs

Piceatannol reduces resistance to statins in hypercholesterolemia by reducing PCSK9 expression through p300 acetyltransferase inhibition

Hyo-Jin Kim [a,b,1], Jangho Lee [a,1], Min-Yu Chung [a], Seungpyo Hong [a], Jae Ho Park [a], Seung-Hyun Lee [c,d], Sahng Wook Park [c,d], Hyo-Kyoung Choi [a,*], Jin-Taek Hwang [a,b,*]

[a] Korea Food Research Institute, Jeollabuk-do, 55365, Republic of Korea
[b] Department of Food Biotechnology, Korea University of Science & Technology, Daejeon, 34113, Republic of Korea
[c] Department of Biochemistry and Molecular Biology, Yonsei University College of Medicine, Seoul, 03722, Republic of Korea
[d] Department of Biochemistry and Molecular Biology, Brain Korea 21 PLUS Project for Medical Sciences, Yonsei University of Medicine, Seoul, 03722, Republic of Korea

ARTICLE INFO

Keywords:
Histone acetyltransferase
PCSK9
Hypercholesterolemia
Statins
Piceatannol

ABSTRACT

The purpose of this study was to investigate the role of piceatannol (PT) in statin (rosuvastatin and simvastatin) resistance and tolerance and its association with PCSK9 expression *via* its p300 inhibitory (p300i) activity. An *in vitro* study was performed using HepG2 cells that were exposed to statins (rosuvastatin or simvastatin) with or without PT in delipidated serum (DLPS) medium. In the statin exposed conditions, *PCSK9* expression was reduced following PT treatment when compared to HepG2 cells w/o PT treatment. Furthermore, no significant difference was observed in the expression of the transcription factors *SREBP2* and *HNF1α*, which regulate *PCSK9* expression. This resulted in low density lipoprotein receptor (LDLR) stabilization and reduced cellular cholesterol levels. This indicates that PT epigenetically controls statin-induced PCSK9 expression. Interestingly, PT attenuated p300 histone acetyltransferase (HAT) activity. Moreover, simulation of PT-p300 binding suggested that PT inhibits p300 as PT could be docked in the p300 HAT domain. Furthermore, inhibition of p300 HAT activity using C-646, a selective p300 inhibitor, or through an siRNA system effectively reduced PCSK9 induction upon statin exposure in HepG2 cells. The chromatin immunoprecipitation (ChIP) assays revealed that PT blocked the recruitment of p300 to the *PCSK9* promoter region. In summary, PT attenuated statin-induced PCSK9 expression by inhibiting p300 HAT activity. Finally, co-administration of simvastatin and PT for 10 weeks further reduced plasma low-density lipoprotein-cholesterol (LDL-C) levels and stabilized the hepatic LDLR protein level compared with those resulting from single treatment of simvastatin in a high-fat diet-induced hypercholesterolemia mouse model. Our findings indicate that PT is a new nutraceutical candidate to reduce the statin resistance and tolerance that occurs in patients with hypercholesterolemia.

1. Introduction

Cholesterol is an essential lipid that plays crucial roles in mammalian cells, such as structural integrity, stability, and cellular organization [1, 2]. Conventionally, the cellular level of cholesterol is tightly regulated to maintain homeostasis, and its imbalance can be triggered by a combination of polygenic predisposition and nutritional factors to result in hypercholesterolemia [3]. Hypercholesterolemia is defined as the presence of abnormally high levels of cholesterol in the blood and is typically considered to be a secondary hyperlipidemia related to various disorders, such as type 2 diabetes (T2D) [4] and obesity [5]. Notably, elevated levels of low-density lipoprotein cholesterol (LDL-C) are known

Abbreviations: CBP, CREB-binding protein; CD, control diet; ChIP, chromatin immunoprecipitation; DLPS, delipidated serum; Fasn, fatty acid synthase; GAPDH, glyceraldehyde 3-phosphate dehydrogenase; PCAF, p300/CBP-associated factor; PT, piceatannol; HAT, histone acetyltransferase; HATi, histone acetyltransferase inhibitor; HDAC, histone deacetylase; HDL-C, HDL cholesterol; HMGCR, 3-hydroxy-3-methylglutaryl-CoA reductase; HNF1α, hepatocyte nuclear factor 1 alpha; LDL-C, LDL cholesterol; LDLR, low density lipoprotein receptor; H&E, hematoxylin and eosin; NAFLD, non-alcoholic fatty liver disease; NE, nuclear extract; PPARγ, peroxisome proliferator-activated receptor-gamma; PCSK9, proprotein convertase subtilisin/Kexin type 9; qRT-PCR, quantitative real-time RT-PCR; SREBP2, sterol regulatory element-binding protein 2; TG, triglyceride; WD, Western diet; WST-1, water-soluble tetrazolium salt.

* Corresponding authors at: Korea Food Research Institute, Jeollabuk-do, Republic of Korea.
E-mail addresses: chkyoung@kfri.re.kr (H.-K. Choi), jthwang@kfri.re.kr (J.-T. Hwang).
[1] These authors contributed equally to this work.

https://doi.org/10.1016/j.phrs.2020.105205
Received 21 July 2020; Received in revised form 4 September 2020; Accepted 11 September 2020
Available online 28 September 2020

to be related with the development of atherosclerotic cardiovascular disease [6].

Statins, which are a primary therapeutic intervention for hypercholesterolemia, are a group of drugs that inhibit 3-hydroxy-3-methylglutaryl coenzyme A (HMG-CoA) reductase (HMGCR). HMGCR is a core enzyme in the rate-limiting step of cholesterol synthesis that catalyzes the conversion of HMG-CoA to mevalonate [7,8]. Although statins have been one of the predominantly prescribed class of drugs to lower LDL-C levels in blood, they have the potential for adverse effects, as with other medications, due to the intermediates produced during the pharmacological processes [9–12]. As such, the biological influences of statins broaden even beyond the direct pathway implicated in mevalonate production, to include ripple effects by modifying the functions of other factors not directly involved in statin pharmacology [10]. The non-mevalonate effects of statins are represented by the increase in proprotein convertase subtilisin/kexin type-9 (PCSK9) [13], which subsequently increases circulating LDL-C levels by accelerating LDL receptor (LDLR) degradation [14].

PCSK9 was first identified as an essential regulator of LDL-C in 2003 [15,16]. PCSK9 is synthesized predominantly in the liver and is secreted into blood with the signal peptide at the N-terminal removed [17]. Secreted PCSK9 binds to cell-surface LDLR and the complex is internalized and then targeted to the lysosome for degradation [18]. Thus, the simultaneous prescription of a PCSK9 inhibitor with statins has been considered as an effective method to overcome the adverse effect and resistance of statins. Evolocumab and alirocumab are human monoclonal antibodies that function as antagonistic PCSK9 inhibitors by binding to PCSK9 and are approved by the US Food and Drug Administration for the treatment of primary hyperlipidemia [19], either alone or in combination with other lipid-lowering therapies, such as statins and ezetimibe, a cholesterol absorption inhibitor [20]. Additionally, nutraceuticals, which use functional foods or dietary supplements with health benefits, have been considered to be effective additions or armamentarium to inhibit PCSK9 expression or activity given their economic advantages and the safety of their use [21]. Mechanistically, many studies have demonstrated that nutraceuticals tend to exert their PCSK9 inhibitory effect in a similar manner. Berberine enhances *LDLR* mRNA expression, resulting in increased LDL-C uptake [22], or suppresses PCSK9 expression at the transcriptional level by impeding the recruitment of HNF1α to the promoter region of the gene [23]. Curcumin also inhibits PCSK9 through the same mechanism as berberine [24]. Additionally, a growing body of evidence indicates that cholesterol homeostasis is controlled by epigenetic mechanisms, such as histone acetylation and DNA methylation, beyond the traditional regulatory schemes [25–27]. However, to the best of our knowledge, few studies have suggested or tested the capacity of nutraceuticals to reduce the statin-induced PCSK9 increase. Furthermore, no epigenetic regulatory mechanism has been identified to overcome the statin resistance and tolerance caused by reduced PCSK9 expression. This is especially true when considering the involvement of nutraceuticals in that mechanism.

During an ongoing screen to identify phytochemical compounds with PCSK9 inhibitory activity and anti-histone acetyltransferase (HAT) activity, we identified piceatannol (PT, trans -3,4,3′,5′-tetrahydroxystilbene or 3,3′,4,5′-tetrahydroxy-trans-stilbene) as a novel PCSK9 inhibitor (PCSK9i) and HAT inhibitor (HATi). PT is a naturally occurring phenolic compound found in various vegetables and fruits, such as grapes, peanuts, and berries [28]. PT, which has a similar structure to resveratrol, is more metabolically stable and has improved bioavailability compared to resveratrol [29]. For this reason, many studies have demonstrated the role of PT in treating cancers, cardiovascular disease (CVD), and other chronic diseases; however, literature regarding PT's beneficial effect in hypercholesterolemia is limited [28,30–32].

In the present study, we investigated the potential of PT as a new PCSK9i and revealed that PT effectively epigenetically reduced statin-induced PCSK9 expression through its anti-HAT activity. PT ameliorated the statin-induced PCSK9 expression in HepG2 cells. In addition, statin-induced PCSK9 expression was positively regulated by p300 HAT, and PT showed an inhibitory effect on p300 HAT activity. Moreover, PT blocked the recruitment of p300 to the *PCSK9* promoter region. In a high-fat diet (HFD)-induced hypercholesterolemia mouse model, co-administration of simvastatin and PT further reduced plasma LDL-C and stabilized hepatic LDLR levels.

2. Materials and methods

2.1. Cell culture and reagents

HepG2 cells (HB-8065) were purchased from the American Type Culture Collection (Manassas, VA, USA). The cells were cultured with high glucose Dulbecco's modified Eagle's medium (DMEM; Corning Inc., Corning, NY, USA) supplemented with 10 % fetal bovine serum (FBS) and 1% antibiotics (Welgene, Daegu, Korea) in a humidified atmosphere of 5% CO_2 at 37 °C. After reaching ≈50 % confluence (day 0), the medium was changed to either DMEM supplemented with FBS or delipidated serum (DLPS) (day 1) that was prepared as previously described [33], and next day, the medium was changed to either FBS or DLPS supplemented DMEM with piceatannol (ChemFaces, Wuhan, China) alone or in combination with rosuvastatin or simvastatin (day 2).

2.2. Statin treatment

Either rosuvastatin or simvastatin was treated the HepG2 cells in delipidated conditions. HepG2 cells were seeded (day 0), and on day 1, the medium was changed to DMEM supplemented with either FBS or DLPS. On day 2, cells were exposed to a statin mixture (statins +50 μM mevalonate) with the replacement of DLPS supplemented media. After additional incubation for 18 h (day 3), the cells were harvested and used for experiments.

2.3. Quantitative real-time RT-PCR

1×10^6 cells were seeded in a 6-well plate and reaching ≈50 % confluence, the medium was changed to either DMEM supplemented with FBS or DLPS, and then next day, cells were treated with PT alone or in combination with statins as the indicated concentrations with replacement of the medium. After 18 h incubation, total RNA was extracted using TRIzol reagent (Invitrogen, Carlsbad, CA, USA), and cDNA were synthesized using. qRT-PCR was performed with SYBR Green PCR master mix (Thermo Fisher Scientific, Waltham, MA, USA) using an I Cycler iQ system (Bio-Rad, Herculus, CA, USA). All reactions were carried out in triplicate using the primers listed in Supplemental Table 1. The relative mRNA expression levels were normalized to those of glyceraldehyde-3-phosphate dehydrogenase (*GAPDH*) mRNA, and calculated using the comparative quantification method.

2.4. Western blotting

Following the cell treatment under the same conditions as used for qRT-PCR, cells were harvested, lysed using lysis buffer (Cell signaling Technology, Danvers, MA, USA) containing protease and phosphatase inhibitors (Roche, Basel, Switzerland), and incubated on ice for 30 min. The lysates were centrifuged at 20,000 × g for 20 min at 4 °C. The extracted proteins were separated on SDS-PAGE and transferred to nitrocellulose membranes. The membranes were blocked in 5% (w/v) non-fat Difco™ skim milk solution in 1 × PBS containing 0.05 % Tween-20 (PBST) for 1 h. The membranes were incubated with the indicated primary antibodies at 4 °C for overnight. All antibodies used in this study were at listed in Supplemental Table 2. Following the incubation with the primary antibodies, the membranes were washed with 1 × PBST, incubated with either the secondary anti-mouse or anti-rabbit horseradish peroxidase-conjugated antibody (Thermo Scientific, Tockford, IL, USA) for 1 h, and visualized using the FUSION-SOLO6s imaging

system (Vilber Lourmat, ZAC de Lamirault, France) with an enhanced chemiluminescence detection reagent (Thermo Scientific).

2.5. PCSK9 measurement

After 70~80 % confluence, HepG2 cells were seeded in a 6-well plate with fresh DMEM (D0). Following incubation for 24 h, the media was changed to either DMEM supplemented with FBS or with delipidated serum (D1). After additional 24 h, the media was then changed to DMEM supplemented with either FBS or DLPS in the presence of PT (D2), followed by incubation for additional 18 h (D3). The media was collected to evaluate extracellular PCSK9 protein level using a commercially-available ELISA kit (STA385; Cell Biolabs Inc., San Diego, CA, USA). In brief, samples and standards were added in 96-well plate pre-coated with antibody against PCSK9, and incubated for 3 h at 37 °C. After washing with wash buffer, the plate was incubated with horseradish peroxidase-conjugated secondary antibody for 1 h. Following additional washing, the plate was incubated with substrate solution for enzymatic reaction. The reaction was stopped by adding a stop solution, and the plate was read at 45 nm in a microspectrometer (Molecular Devices, Sunnyvale, CA, USA). PCSK9 was normalized to total protein contained in the media, which was measured using Bradford assay (Bio-Rad Laboratories; Hercules, CA, USA).

2.6. LDLR protein stability

HepG2 cells were cultured as described above, and seeded in 6-well plate (D0). HepG2 cells were then incubated with fresh DMEM supplemented with DLPS (D1), followed by a treatment with either bafilomycin A1 (BA1; B1739; Sigma-Aldrich) at 0 or 50 nM or PT at 0 or 40 μM (D2). After 24 h incubation (D3), the cells were washed with cold PBS, harvested, and centrifuged (1200 rpm, 3 min).

2.7. Filipin staining assay

HepG2 cells were cultured as described above, and seeded at 3×10^4 cells/well in a 96-well plate (day 0). The medium was changed to DMEM supplemented with DLPS (day 1). Next day, the cells were exposed to a statin mixture (statins +50 μM mevalonate) with the replacement of DLPS supplemented media (day 2). After additional incubation for 18 h, the cells were washed with PBS for 3 times and then fixed with 3.7 % paraformaldehyde for 1 h at room temperature. The cells were rinsed with PBS for 3 times, followed by incubation with 100 μL of 1.5 mg glycine/mL in PBS for 10 min at room temperature to remove the residual paraformaldehyde. Filipin staining was conducted for 2 h at room temperature using 50 μg/mL of filipin solution in 10 % FBS solution in PBS. After completion of filipin staining, the cells were rinsed with PBS for 3 times, and fluorescence intensity was measured at 360/480 nm (exciation / emission) using SpectraMax M2 microplate reader (Molecular Devices, Sunnyvale, CA, USA).

2.8. siRNA transfection

The siRNA sets were obtained from Genolution (Seoul, Korea): p300 siRNA (sip300), sense 5′−CCUCGUGCCGUUCCAUCAGGUAGUU-3′, antisense 5′-CUACCUGAUGGAACGGCACGAGGUU -3′. 50 pmol of a non-specific siRNA (NC) or the sip300 was transiently transfected using Lipofectamine RNAiMax system into the cells according to the manufacturer's guide.

2.9. Histone acetyltransferase activity measurement

For HAT assays based on cell free condition, either HeLa nuclear extract or p300 recombinant enzyme (BioVision Biotehnology, Milpitas, CA, USA) was used as the HAT enzyme source. HAT activities were assessed using a commercially available kit according to the manufacturer's instrument (BioVision Biotechnology). IC50 values were calculated using Prism 7 software (Version 7.0.4; GraphPad Software Inc., CA, USA). To investigate the inhibitory effect of PA in the cell, cytosol and nuclear were respectively fractionized with Nuclear Extraction Kit (Abcam, Cambridge, UK) in accordance with the manufacturer's protocol and each nuclear faction was used for the HAT assays.

2.10. Animal experiments

Male C57/BL6J mice (12-week-old) were purchased from Central Lab Animal Inc. (Seoul, Korea) and housed in a light-controlled room kept at a temperature of 23 ± 3 °C and a relative humidity of 50 ± 5% with free access to water and a diet. The protocol for the care and use of animals was approved by the Institutional Care and Use Committee at Korea Food Research Institute (#KFRI-M-17,010). After 1-week acclimation, 24 mice were fed with a high fat diet (HFD, Research Diet Inc. New Brunswick, NJ, USA) for 16 weeks. Mice were then randomly divided into 3 groups as follow: 1) HFD group (n = 8), 2) HFD with simvastatin (20 mg/kg body weight, n = 8), and 3) HFD with simvastatin (20 mg/kg BW) and piceatannol (40 mg/kg body weight). Intake dosage and preparation method for simvastatin was determined as described previously with minor modification [36,34,35]. Simvastatin and piceatannol were provided by oral gavage, and PBS with 3.3 % ethanol and 5% 0.1 N NaOH, which together adjusted to pH 7, was used as a vehicle. Body weight was monitored every week. After 10-week treatment, mice were sacrificed after overnight fasting (10−12 hours). Blood was collected from retro-orbital sinus. Serum was obtained by centrifugation (430 xg, 10 min) and analyzed (GC Lab Cell, Yongin, Korea). Liver was harvested, washed with saline solution, and stored at −80 °C for further analysis.

2.11. Hematoxylin and eosin staining

The specimens fixed in 4% formalin, embedded in paraffin, and cut into 4–5 μm-thick sections, which were stained with hematoxylin and eosin (H&E). Lipid droplets were assessed by microscopic observation using an LEICA DM500 microscope (LEICA, Wetzlar, Germany), and captured by LEICA ICC50 HD (LEICA).

2.12. Docking simulation

A crystal structure of p300 HAT domain was retrieved from the Protein Data Bank (http://www.rsch.org/pdb/) (PDB ID: 4PZB). The structure contains an acetyl-CoA, and a Y1467 F mutation was introduced near the acetyl groups of acetyl-CoA. The phenylalanine at residue 1467 was mutated back into the tyrosine using the muatagenesis module in PyMol (The PyMOL Molecular Graphics System, Version2.2.2, Schrödinger, LLC.). The structure of piceatannol and C-646 were retrieved from PubChem, with CID of 667,639 and 1285941, respectively [37]. The structures were converted into MOL2 and PDBQT formats using the Open Babel Package (Version 2.4.1) [38] and AutoDock Tools (Version 1.5.7) [39]. The ligand molecules were docked in the 30 Å cubic box placed near the acetyl-CoA binding site of the HAT domain using AutoDock Vina (Version 1.14.2, the Scripps Research Institute, La Jolla, CA, USA) [40]. The docking poses of the lowest docking scores were inspected and illustrated by using PyMol (The PyMOL Molecular Graphics Systems).

2.13. Chromatin immunoprecipitation assay

Cells (5×10^6) were seeded in 100-mm dishes and treated with PT in presence or absence of simvastatin at the indicated concentrations for 18 h to reach approximately 70 % confluence (~2×10^8 cells). A chromatin immunoprecipitation (ChIP) assay was carried out by following a previously described method [41]. Briefly, cells were initially treated with

PBS containing 1% formaldehyde for 10 min, washed twice with cold PBS, and then incubated with 100 mM Tris (pH 9.4) and 10 mM DTT at 30 °C for 15 min. The cells were then rinsed twice in PBS and resuspended in 600 μL of SolA [10 mM HEPES (pH 7.9), 0.5 % NP-40, 1.5 mM $MgCl_2$, 10 mM KCl, and 0.5 mM DTT] by pipetting. After a short spin, the pellets were resuspended in SolB [20 mM HEPES (pH 7.9), 25 % glycerol, 0.5 % NP-40, 0.42 M NaCl, 1.5 mM $MgCl_2$ and 0.2 mM EDTA] containing protease inhibitors, followed by vigorous pipetting to extract nuclear proteins. After centrifugation at 13,000 rpm for 30 min, the nuclear pellets were resuspended in immunoprecipitation buffer [1% Triton X-100, 2 mM EDTA, 20 mM Tris−HCl (pH 8.0), 150 mM NaCl and protease inhibitors], and chromatin was broken by micrococcal nuclease digestion using a Pierce Agarose ChIP Kit (Thermo Fisher Scientific) into fragments of 0.5–1.0 kb average length. The ChIP assays were then preformed using the indicated antibodies essentially as described (Supplemental Table 2) but without SDS in all buffers. The primers used for ChIP assays are listed in Supplemental Table 1. All reactions were normalized relative to input activities and are presented as the mean ± SD of three independent experiments.

2.14. Statistical analysis

Data were analyzed using either students' *t*-test or one-way analysis of variance with Tukey's multiple comparison test, and values were expressed at the mean ± SD. Statistical analysis was carried out using the SPSS software (Version 20; SPSS Inc., Chicago, IL, USA). Difference were considered statistically significant at $p < 0.05$.

3. Results

3.1. PT suppresses delipidation-induced intra-/extra-cellular PCSK9 levels and stabilizes LDLR by downregulating SREBP2 and HNF1α transcription factors

It is well established that LDLR and PCSK9 are the key factors that ultimately control steady-state serum LDL-C levels [42]. Thus, we hypothesized that PT would lower LDLR and PCSK9 levels. To test this hypothesis, we measured the protein and mRNA expression levels of LDLR and PCSK9 following PT treatment using the DLPS system. First, we compared the effect of PT with resveratrol, which is known to inhibit PCSK9. As shown in supplementary Fig. S1, PCSK9 inhibition and LDLR

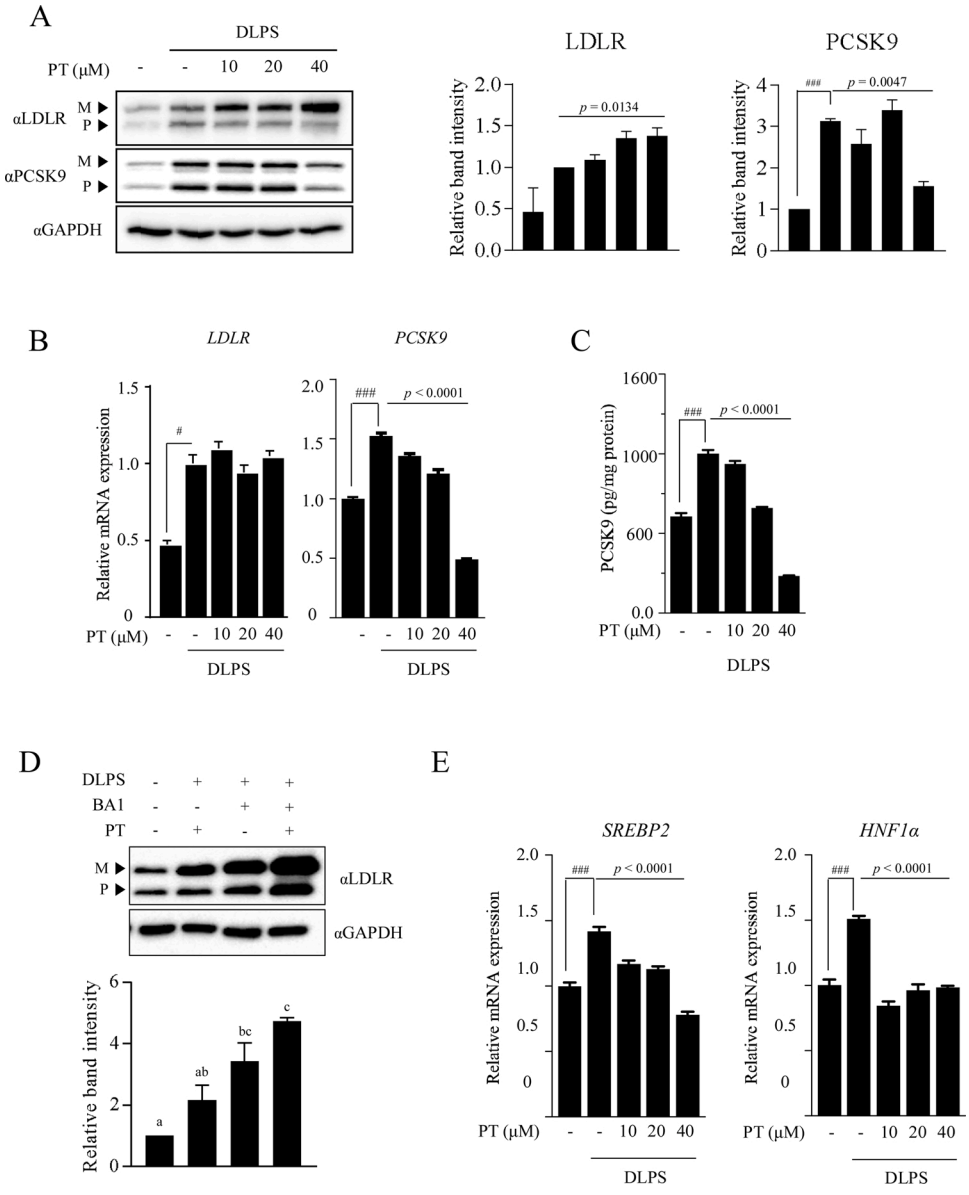

Fig. 1. PT abrogated *PCSK9* gene expression through inhibiting the transcription factors *HNF1α* and *SREBP2*, and stabilized LDLR through obstruction of lysosomal degradation. (A) PT decreased PCSK9 and increased LDLR expression levels. HepG2 cells were exposed to DLPS with or without PT at the indicated concentrations for 18 h. Total protein was extracted from the harvested cells and used for western blotting to detect the indicated proteins. ###$p < 0.001$. (B) PT decreased *LDLR* and *PCSK9* mRNA expression levels. HepG2 cells were treated with PT at the indicated concentrations under the DLPS condition for 18 h; mRNA expression of *LDLR* and *PCSK9* was measured by qRT-PCR. The values presented are the means ± SD of three independent experiments; ###$p < 0.001$. (C) PT reduced the PCSK9 protein level in medium. HepG2 cells were treated with PT at the indicated concentrations with DLPS. After 18 h, the medium was collected and used for measuring PCSK9 levels. (D) PT blocked the lysosomal degradation of LDLR. HepG2 cells were exposed to the DLPS condition with 40 μM PT or 10 μM BA1 alone or in combination for 24 h. The cells were harvested and total protein was extracted. LDLR expression was measured using western blotting with a specific antibody (upper panel). Means with different superscript letters are significantly different ($p < 0.05$) (lower panel). (E) PT reduced *SREBP2* and *HNF1α* mRNA expression levels. HepG2 cells were treated with PT at the indicated concentrations under the DLPS condition for 18 h. mRNA expression of *SREBP2* and *HNF1α* was measured by qRT-PCR. The values presented are the means ± SD of three independent experiments; ###$p <$ 0.001.

stabilization were relatively higher following PT treatment than after resveratrol treatment. DLPS triggered the stabilization of LDLR and PCSK9. However, following PT treatment, LDLR expression levels were significantly increased in a dose dependent manner. In contrast, the stabilized PCSK9 levels in response to DLPS were destabilized upon PT treatment (Fig. 1A). To determine whether the changes in expression of these two proteins were due to changes in mRNA production, we examined the mRNA expression levels of *LDLR* and *PCSK9* using qRT-PCR under the same conditions as western blotting. Interestingly, the transcription of *PCSK9* was dramatically suppressed by PT treatment in a dose-dependent manner (Fig. 1B, right panel) while the transcription of *LDLR* was unaffected by PT treatment (Fig. 1B, left panel). To determine whether the reduced levels PCSK9 in the cell also influenced PCSK9 levels in the blood, secreted-PCSK9 concentrations were detected. As shown in Fig. 2C, extracellular PCSK9 concentrations were markedly decreased following PT treatment, and PT treatment caused

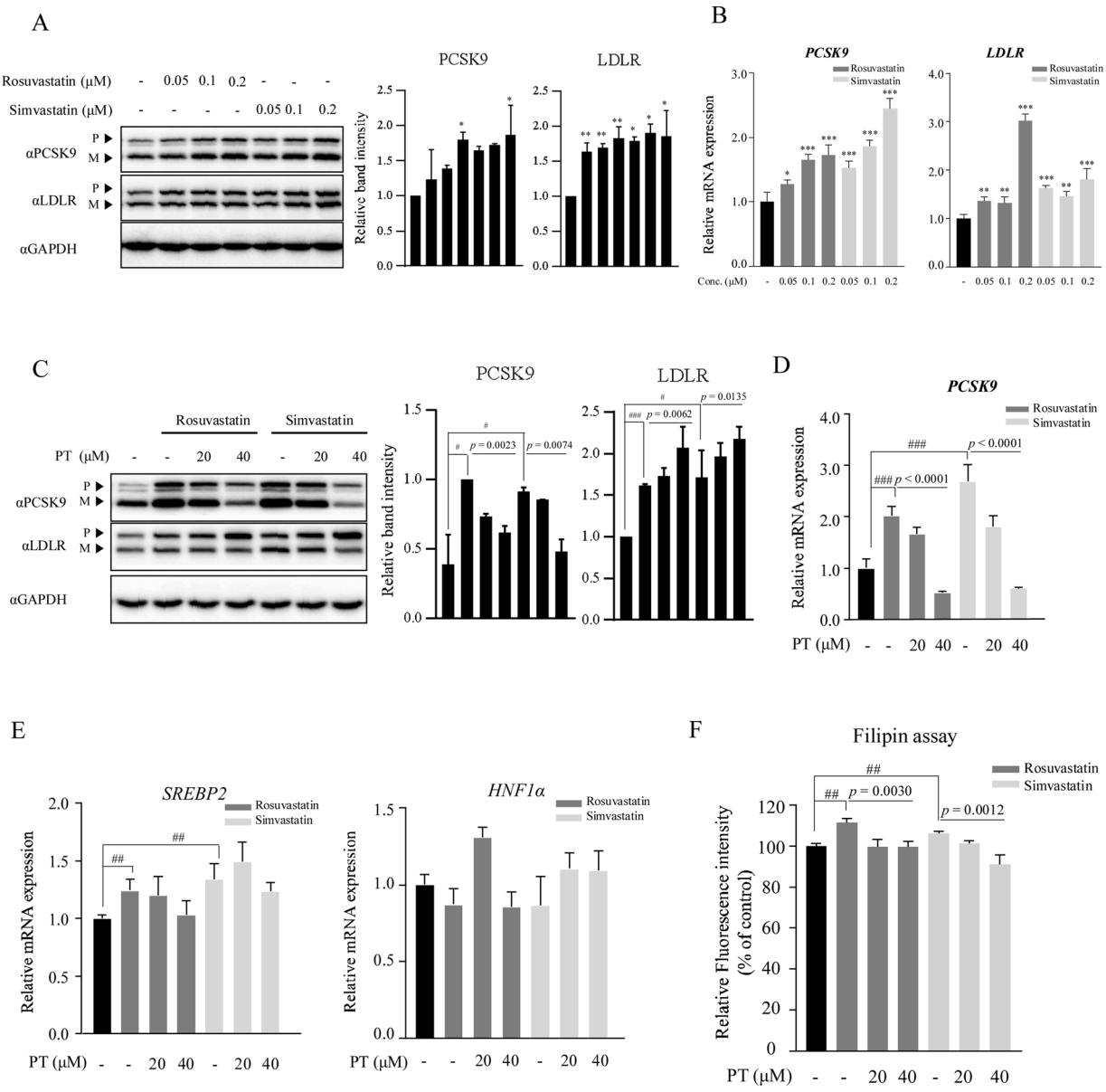

Fig. 2. PT induced PCSK9 reduction and LDLR stabilization regardless of the transcription factor, *SREBP2* and *HNF1α*, under treatment with the DLPS-statin combination. (A, B) Statins increased PCSK9 and LDLR levels in a dose-dependent manner. HepG2 cells were treated with either rosuvastatin or simvastatin at the indicated concentrations for 18 h. RNA or total protein was extracted from the harvested cells, and PCSK9 or LDLR expression was measured using western blotting (A) or qRT-PCR (B). The values presented are the means ± SD of three independent experiments; $*p < 0.05$, $**p < 0.01$, and $*** p < 0.001$. (C) PT controlled the statins-induced PCSK9 increase, resulting in more stabilized LDLR. HepG2 cells were treated with either 0.2 μM rosuvastatin or 0.2 μM simvastatin in the presence or absence of PT at the indicated concentrations for 18 h. Total protein was extracted from the harvested cells and used for western blotting to determine LDLR and PCSK9 protein levels; $\#p < 0.05$ and $\#\#\#p < 0.001$. (D) The statins-induced *PCSK9* mRNA increase was reduced following PT treatment. PT was applied with either 0.2 μM rosuvastatin or 0.2 μM simvastatin to HepG2 cells for 18 h. RNA was extracted, reverse-transcribed to cDNA, and then used in qPCR to measure *PCSK9* mRNA levels. The values presented are the means ± SD of three independent experiments. $***p < 0.001$ and $\#p < 0.05$. (E) PT did not affect *SREBP2* and *HNF1α* expression in the statin-exposed condition. HepG2 cells were exposed to 0.2 μM rosuvastatin or 0.2 μM simvastatin with or without PT for 18 h. RNA was extracted from the harvested cells, and *SREBP2* and *HNF1α* expression levels were measured using qRT-PCR. The values presented are the means ± SD of three independent experiments; $**p < 0.01$, $***p < 0.001$, and $\#p < 0.05$. (F) PT reduced free cholesterol in cells to a greater extent than statin. HepG2 cells were exposed to 0.2 μM rosuvastatin or 0.2 μM simvastatin with 40 μM PT for 24 h. To measure the amount of cholesterol in the plasma membrane, cells were stained with the fluorescent dye Filipin III, and the fluorescence intensity was measured using a fluorescence microplate reader.

similar changes in the protein and mRNA levels of *PCSK9*. To determine the mechanisms through which PT regulates LDLR and PCSK9, we hypothesized that PT could affect LDLR stabilization by blocking its lysosomal degradation given the results presented in Fig. 1A and 1B. To the test our hypothesis, a lysosomal protease inhibitor, BA1, was used. As shown in D, LDLR expression was stabilized by PT treatment, although the stabilization was relatively lower than that caused by BA1 alone. However, LDLR was noticeably stabilized when a combination of BA1 and PT was used. Based on previous results, changes in the intracellular or extracellular PCSK9 levels were mediated by the PT-mediated regulation of PCSK9 mRNA expression. Thus, the mRNA expression of two transcription factors, *SREBP2* and *HNF1α*, which are known to regulate transcription of *PCSK9,* were measured using qRT-PCR. As shown in Fig. 1E, the increase in *SREBP2* and *HNF1α* mRNA levels in response to DLPS were significantly reduced upon PT treatment. Taken together, PT suppressed the intracellular or extracellular PCSK9 levels by down-regulating the transcription factors *SREBP2* and *HNF1α*, and stabilized LDLR expression levels by inhibiting lysosomal degradation.

3.2. PT ameliorates statin resistance by reducing PCSK9 expression and stabilizing LDLR

Although PT suppressed mRNA expression of *HMGCR*, a key enzyme for mevalonate biosynthesis, in the DLPS system (Supplementary Fig. S2), from the results obtained, we inferred that PT administered for hypercholesterolemia could overcome non-mevalonate side-effects of statins by suppressing PCSK9 and further stabilizing LDLR. To further explore this scenario, PT was administered with rosuvastatin or simvastatin in the DLPS condition. Statins, rosuvastatin or simvastatin, upregulated PCSK9 and LDLR protein and mRNA expression in the presence of mevalonate (Fig. 2A, B). Following treatment with a combination of each statin and PT, not only was LDLR clearly stabilized but PCSK9 was also degraded in a PT-concentration dependent manner (Fig. 2C), without regard to the inhibitory effect of PT on the mRNA expression of *HMGCR* and *HMGCS2*, which encode mevalonate synthesis enzymes (Supplementary Fig. S3). To determine if these results had the same underlying mechanism as that of the DLPS system (Fig. 1), *PCSK9* mRNA expression was detected with the indicated conditions using qRT-PCR (Fig. 2D). Each statin induced *PCSK9* mRNA expression, and this was significantly reduced upon PT treatment (Fig. 2D). Interestingly, following PT treatment, there was a noticeable difference in the regulation of SREBP2 and HNF1α under statin treatment compared to DLPS treatment alone. As shown in Fig. 2E, a combination of PT and statins did not affect the regulation of SREBP2 and HNF1α. To determine whether the PT-derived intracellular actions do indeed lower the cholesterol, the classical filipin cholesterol staining was adapted. Intracellular cholesterol was increased by statin treatment and was conspicuously repressed following PT treatment (Fig. 2F) These results

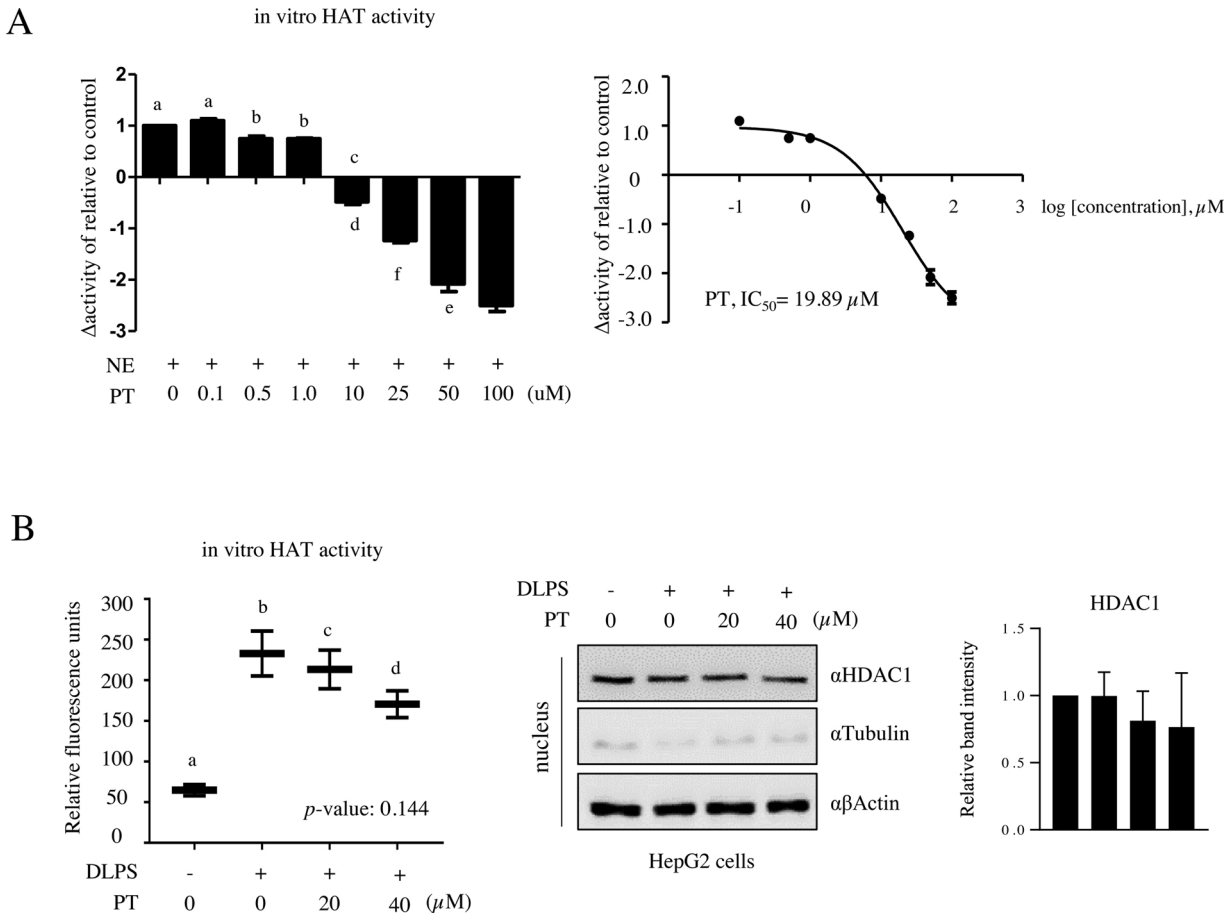

Fig. 3. PT inhibited histone acetyltransferase activity. (A) PT is a potential HAT inhibitor. A colorimetric assay using a cell-free system was conducted to measure HAT activity in the presence of PT at the indicated concentrations. The results are presented as the relative fold change to the control (NE alone) sample, which was incubated without PT (left panel). The IC_{50} value of PT for inhibition of HAT activity was calculated using Prism software (right panel). Means with different superscript letters are significantly different ($p < 0.05$) (left panel). (B) HAT activity in nuclear extracts of HepG2 cells was also inhibited following PT treatment. The HAT activity was measured in NE from HepG2 cells. PT was treated to HepG2 cells for 24 h, and the nuclear fraction was obtained and then used as the enzyme source to measure HAT activity. Activity in each group is presented as a percentage relative to that in the control group. The values presented are the mean ± SD of three independent experiments. Means with different superscript letters are significantly different ($p < 0.05$) (left panel). To confirm the fraction, western blotting was carried out; HDAC1 and tubulin were used as nuclear and cytosol markers, respectively (right panel).

supported our hypothesis that PT may improve the statin-induced non-mevalonate effect by suppressing PCSK9 and stabilizing LDLR independent of other transcription factors.

3.3. PT is a potent novel histone acetyltransferase inhibitor

Previously, we confirmed that the PT-mediated regulation of *PCSK9* under statin treatment conditions was independent of the transcription factors, *SREBP2* and *HNF1α*. Therefore, we deduced that the control of the two genes was likely achieved by epigenetic mechanisms. To assess this, we initially measured histone acetyltransferase activity in a cell-free system following PT treatment at the indicated concentrations. In this system, HeLa cell nuclear extract (NE) was used as the source of HAT enzymes. As shown in Fig. 3A (left panel), PT significantly inhibited the global HAT activity with an IC_{50} value of 19.89 μM (right panel). To determine if HAT enzymes are truly implicated in the statin-induced non-mevalonate effect following PT treatment, we re-examined HAT activity in cells under the indicated conditions and measured total HAT activity in isolated nuclear fractions. In the DLPS and statin co-treated groups, HAT activity was significantly higher than in the DLPS-only treated group, and this increase in HAT activity was significantly inhibited by PT treatment (Fig. 3B, left panel). Western blotting confirmed successful cell fractionation (Fig. 3B, right panel). These results indicate that PT is a potent novel histone acetyltransferase inhibitor (HATi), and PT may be able to control statin-induced PCSK9 expression through this novel function.

3.4. PT suppresses statin-induced PCSK9 expression by inhibiting p300

Previous studies have demonstrated that p300, a representative HAT, is transcriptionally regulates *LDLR* and *PCSK9* [43]. Thus, we investigated whether PT modulates p300 activity. As shown in Fig. 4A, as expected, p300 activity was significantly inhibited by PT in a dose/time dependent manner. Next, we investigated the possibility for binding

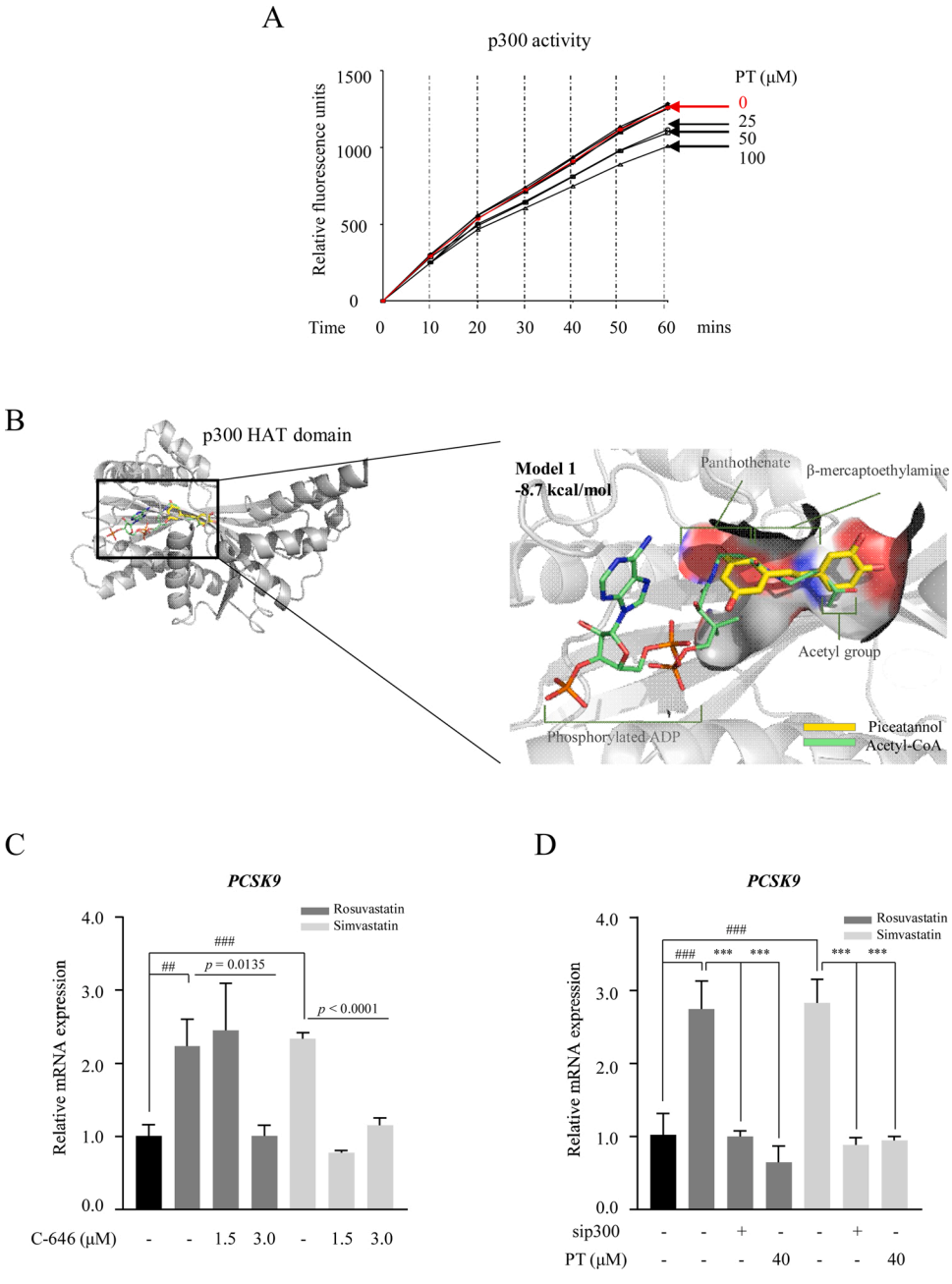

Fig. 4. PT suppressed statins-induced *PCSK9* expression through inhibition of p300 HAT activity by docking in the p300 HAT domain. (A) PT showed a p300 acetyltranferase inhibitory effect. The P300 enzyme-specific anti-HAT activity of PT was measured using a recombinant protein. A colorimetric assay using a cell-free system was conducted to measure p300 HAT enzyme activities in the presence of PT at the indicated concentrations. The results are presented as relative fold changes to a control sample, which was prepared without PT. The values presented are the means of three independent experiments. (B) PT was expected to bind the p300 catalytic pocket at the HAT domain. The most likely PT-p300 docking is presented (left panel), and the docking site is expanded (right panel). The target protein (p300) is represented by a gray surface area and the ligands (PT or acetyl-CoA) are represented by sticks. When selecting the lowest energy ligand in the cluster, free energy (lowest energy + ($-kT\ln N$), k: Boltzman constant, T: Kelvin temperature, N: number of structures in each cluster) was used to account for the number of ligands in the population. (C) The inhibition of p300 activity reduced statins-triggered *PCSK9* induction. HepG2 cells were exposed to either rosuvastain or simvastatin with or without (w/o) C-646, a p300-selective inhibitor for 18 h. RNA was extracted, and cDNA was synthesized and then used for qPCR. The values presented are the means ± SD of three independent experiments; $##p < 0.01$ and $###p < 0.001$. (D) P300 knockdown using siRNA reduced statins-induced *PCSK9* expression; 50 pmol p300 siRNA was transiently transfected into HepG2 cells, which were treated with statins the next day for 18 h. RNA was extracted, and cDNA was synthesized and then used for qPCR. The values presented are the means ± SD of three independent experiments; $###p < 0.001$ and $***p < 0.001$.

between PT and p300 through a docking simulation. In the docking model, the two aromatic rings of PT were placed on the HAT domain of p300 surrounded by the hydrophobic residues I1395, Y1397, L1398, I1435, Y1446, L1463, and Y1467, where the β-mercaptoethylamine and pantothenate moieties of acetyl-CoA bind (Fig. 4B). The polar hydroxyl groups of PT were located at the ends of the channel that are exposed to solvent. Corresponding locations are occupied by the acetyl and phosphate groups of acetyl-CoA in its complex structures. The hydrophobic and hydrophilic pattern of PT moieties were matched to that of the p300 HAT domain, and this was consistently observed in the top four docking structure (Supplementary Fig. S4). The data indicate that PT may control the activity of p300 by disturbing the binding of acetyl-CoA to the p300 HAT domain. To establish the relationship between the *PCSK9* mRNA expression and p300 activity, C-646, a specific p300/CBP inhibitor, and p300 siRNA were used. Cells were incubated with statins in the presence or absence of C-646 under DLPS-exposed conditions, and *PCSK9* mRNA expression was measured. As shown in Fig. 4C, the increased mRNA expression of *PCSK9* caused by statins was significantly reduced by inhibiting p300 with C-646. To confirm this, p300 was selectively knocked down using siRNA, and *PCSK9* expression was measured. Remarkably, the statins (rosuvastatin and simvastatin) failed to increase *PCSK9* expression upon p300 knockdown, and *PCSK9* was expressed at a similar level to that of the PT-treated condition (Fig. 4D). Altogether, these data indicated that p300 is responsible for the statin-induced increase in *PCSK9* expression, and PT effectively blocks this by attenuating p300 activity by binding the p300 HAT domain (Fig. 5).

3.5. PT abrogates p300 recruitment to the PCSK9 promoter region

The p300-induced modulation of lysine acetylation on histones in promoter regions triggers conformational changes in DNA, influencing the transcriptional activity of genes [44]. To elucidate whether the changes in *PCSK9* mRNA expression are regulated by recruitment of p300 to the *PCSK9* promoter region, we performed chromatin immunoprecipitation (ChIP) assays. As shown in Fig. 6, simvastatin treatment enhanced p300 enrichment at the PCSK9 promoter region (-337 ~ -278 bp), and this was effectively diminished upon treatment with 40 μM PT. Our findings indicate that PT may induce hypoacetylation of histones around the PCSK9 promoter region by reducing p300 binding in the region, which consequently affects *PSCK9* mRNA expression.

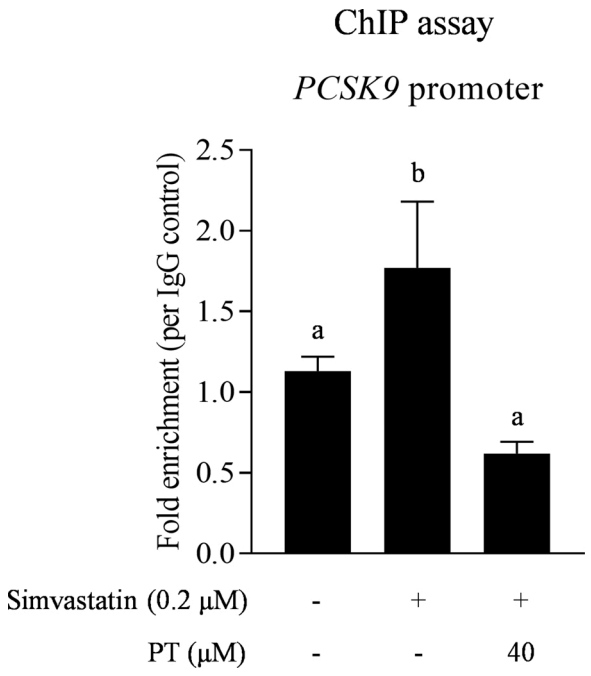

Fig. 5. PT blocked simvastatin-induced p300 recruitment to the *PCSK9* promoter region. HepG2 cells were treated with 0.2 μM simvastatin in the presence or absence of PT at the indicated concentrations for 24 h, and ChIP assays were performed using the indicated antibodies. The precipitated samples were analyzed by qRT−PCR. The values presented are the means ± SD of three independent experiments. Means with different superscript letters are significantly different ($p < 0.05$).

3.6. PT overcomes stain side effects in HFD-fed mice

To confirm whether PT effectively attenuates the statin-induced PCSK9 increase and consequently stabilizes LDLR, as well as reduces the LDL-C level in blood, we conducted an *in vivo* experiment with an HFD mouse model. In brief, mice were fed an HFD for 16 weeks, and were then treated with either simvastatin alone or with the simvastatin-PT combination for 10 weeks. As shown in Fig. 6A and 6B, there were no significant differences in body weight, weight gain, and fat mass among the groups. However, the liver mass was effectively reduced in the treatment groups with either simvastatin alone or the simvastatin-PT combination compared with that of the control group (no treatment). Interestingly, the simvastatin-PT combination most strongly suppressed the LDL-C and total-C levels in the blood compared with the other two groups (Fig. 6C). No change in the triglyceride level was detected among groups (Fig. 6C, right panel), and there were also no differences in the toxicity indicators such as ALP, ALT, and AST among groups (Supplementary Fig. S5). Finally, LDLR was expressed at the highest level in the simvastatin-PT combination group (Fig. 6D), which verified the *in vitro* effect that reducing the LDL-C level following PT administration was mediated through suppressing stain-induced LDLR degradation. Taken together, these results confirmed that PT reduced the LDL-C level by enhancing LDLR stabilization, suggesting that the side effects of statins can be overcome through PT administration to consequently improve the therapeutic efficacy of statin.

4. Discussion

It is well known that statins are the core HMG-CoA inhibitors used in pharmacological therapy to treat hypercholesterolemia [45]. Furthermore, they have been proven to be safe for use in reducing the occurrence of stroke, peripheral vascular disease, coronary disease, and LDL-C levels [46]. Despite the various benefits of statins, they occasionally cause resistance or intolerance in patients due to differences in protein expression across various target pathways that are unrelated to its pharmacokinetic mechanisms. These include alterations in HMG-CoA reductase, as well as in diverse factors implicated in cholesterol biosynthesis and the lipoprotein metabolic pathway [47]. PCSK9 is also known to be a major factor that induces the non-mevalonate effects that cause statin resistance and intolerance. Rashid et al. [48] reported that administration of statin to *Pcsk9* knockout mice led to a substantial increase in hepatic LDLR protein and reduction of plasma LDL-c levels. For this reason, PCSK9i, such as evolocumab, have been considered as novel medications for lowering LDL-C levels in patients who are unable to achieve normal levels of LDL-C with statins [49]. Our study suggested that PT could be a novel potent PCSK9i and elucidated its mechanism of action at the molecular level.

Initially, we found PT to have powerful anti-lipogenic effects (Supplementary Fig. S6) during an ongoing screening study using 3T3-L1 preadipocytes to identify phytochemicals exhibiting anti-obesity effects. To confirm the efficacy of PT, we evaluated whether PT can improve various pathological phenomena implicated in obesity following ingestion of 0.025 % or 0.05 % PT for 12 weeks in a WD-induced obesity model (Supplementary Fig. S7). Consistent with previous reports [50,51], our data showed a decrease in weight gain, liver mass, retroperitoneal and epididymal fat mass, the reduction of the size of epididymal fat cells, and inhibition of lipid accumulation in hepatocytes. Sufficient evidence has been accumulated to support the claim

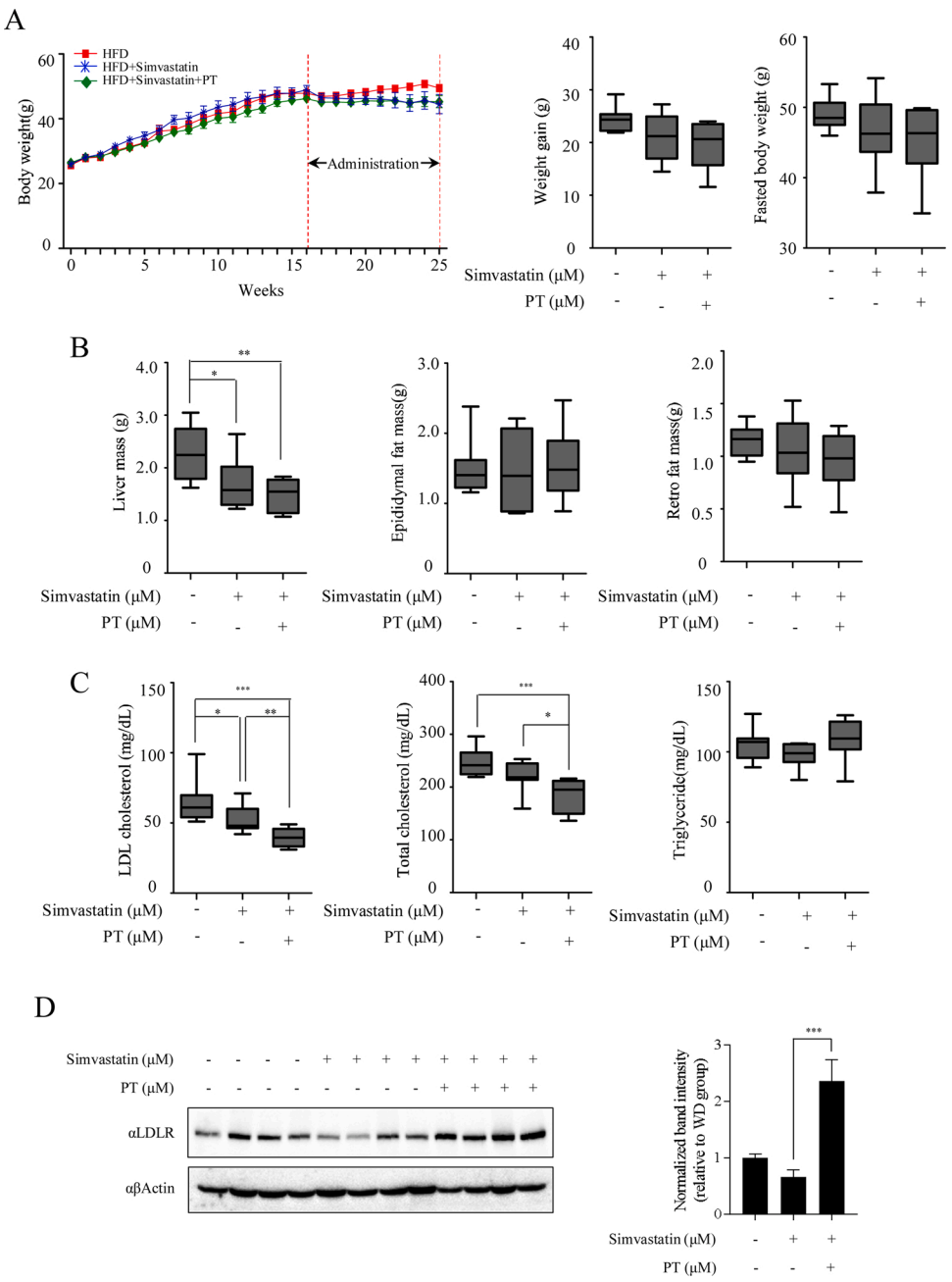

Fig. 6. PT regulates HFD-mediated pathological features in obese mice. (A) Body weight changes, weight gain, and fasted body weight in mice fed the HFD alone, HFD feeding followed by simvastatin administration (20 mg/kg BW), or HFD feeding followed by combined simvastatin (20 mg/kg BW) and PT (40 mg/kg BW) administration (n = 8/group). Mice were fed the HFD for 16 weeks, and then treated with either simvastatin or simvastatin + PT for an additional 10 weeks. Simvastatin or simvastatin + PT did not affect body weight changes, weight gain, or final body weight in obese mice. (B) Masses of tissues (liver and fat) from mice fed the HFD alone, HFD with simvastatin (20 mg/kg BW), or HFD with simvastatin (20 mg/kg BW) and PT (40 mg/kg BW; n = 8/ group). Simvastatin and simvastatin + PT significantly attenuated the liver mass, but not fat mass, in obese mice compared to HFD-fed mice. (C) Blood lipid profile from mice fed the HFD alone, HFD with simvastatin (20 mg/kg BW), or HFD with simvastatin (20 mg/kg BW) and PT (40 mg/kg BW; n = 8/group). Both simvastatin and simvastatin + PT significantly attenuated LDL cholesterol in obese mice (left panel), and simvastatin + PT significantly reduced total cholesterol compared to HFD-only or simvastatin-treated obese mice (middle panel). The triglyceride (TG) level was not affected by diet, simvastatin, or PT. The values presented are the means ± SD;*$p < 0.05$, **$p < 0.01$, ***$p < 0.001$. (D) Hepatic LDLR levels in mice fed the HFD alone, HFD with simvastatin (20 mg/kg BW), or HFD with simvastatin (20 mg/kg BW) and PT (40 mg/kg BW; n = 4/group). Simvastatin+PT significantly stabilized hepatic LDLR in obese mice. The LDLR protein levels in the mouse liver were immunoblotted by western blotting (left panel) and quantified by Image J software (right panel). The values presented are the means ± SEM (n = 4);***$p < 0.001$.

that PT helps overcome insulin resistance in high-fat diet-induced T2DM mice [52,53]. Therefore, in this study, we noted the PT-induced lowering of LDL-C given that the previously mentioned efficacy has already been identified.

Following PT treatment in the DLPS-treated HepG2 model, we found that PT downregulated PCSK9 expression by downregulating the transcription of the transcription factors *SREBP2* and *HNF1α*, which are responsible for *PCSK9* mRNA expression. In 2010, the strong induction of PCSK9 expression by *SREBP2* and *HNF1α*was reported [54]. This was further supported by additional reports that circulating PCSK9 and LDL-C levels were reduced by liver-specific knockdown of HNF1α [55] and that *SREBP2* deletion in mouse hepatocytes led to the preferential inactivation of *PCSK9* [56]. Many studies have identified that *SREBP2* controls LDLR expression to maintain cholesterol homeostasis [57,58]. As expected, *LDLR* mRNA expression was also decreased in a PT-treated group in a concentration dependent manner, similar to *SREBP2* expression. However, it is important to note that LDLR exhibited increased protein expression depending on the concentration of PT, unlike its mRNA expression, indicating that PT regulates LDLR at the post-translational level. In addition, our data, which showed dramatic LDLR stabilization following PT treatment with BA1, supported this notion. Based on these results, we inferred that PT-triggered LDLR expression could be regulated through the following two mechanisms: i) PT could directly stabilize LDLR at the post-translational level itself; ii) PT could indirectly stabilize LDLR by reducing PCSK9 expression. PCSK9 binds to LDLR and makes it a target for lysosomal degradation in cells, which consequentially causes plasma clearance of LDL-C from the blood to fail [44,45]. A previous study showed that *Pcsk9* knockout resulted in an increase in hepatic LDLR protein independent of its mRNA alteration, and improved plasma LDL clearance in mice [48]. Therefore, the inhibition of either PCSK9 mRNA or protein expression, by monoclonal antibodies or small molecules, respectively, is a compromising strategy for hypercholesterolemia therapy [59]. Additionally, we cannot rule out the possibility of controlling the E3 ubiquitin ligase, IDOL (inducible

degrader of the LDLR), by PT. IDOL accelerates LDLR degradation through the ubiquitination of its C-terminus [60]. Thus, the regulation of IDOL by PT or obstruction of IDOL-induced LDLR degradation through direct binding of PT to the LDLR ubiquitination site is also a possible mechanism by which PT could stabilize LDLR.

Furthermore, the PT-induced reduction in PCSK9 and stabilization of LDLR led us to establish the hypothesis that PT application in hypercholesterolemia overcomes statin resistance and intolerance. Indeed, our results demonstrated that in the statin-treated DLPS group, PT completely inhibited PCSK9 expression and stabilized LDLR to a greater degree than in the DLPS treated group. However, *PCSK9* mRNA expression was clearly suppressed in the absence of changes in *SREBP2* and *HNF1α* expression, demonstrating that the reduction in PCSK9 expression is likely mediated by a different mechanism than that of lipid depletion. In this regard, we believed that in the statin-treated conditions, PT regulated *PCSK9* epigenetically.

Controlling gene expression by changing histone acetylation patterns of a gene is a representative epigenetic mechanism and is regulated by histone acetyltransferases (HATs) and histone deacetylases (HDACs) [61]. There are now several known HAT inhibitors (HATi) derived from nutrients, such as EGCG [62], anacardic acid [63], curcumin [64], and tannic acid [65], with safety profiles that suggest HATs are a plausible target for preventive or therapeutic agents [66,67]. Although there was a report demonstrating the potential of PT as a novel HDAC inhibitor (HDACi) [68], to the best of our knowledge, no studies have suggested its potential as a HATi. In this present study, we found that PT functioned as a novel HATi against p300. By extension, to address the mode of action of PT as a HATi, we simulated a possible p300-PT docking model, which revealed that PT interacts with the HAT domain of p300. The autoacetylation of the p300 HAT domain, which is dependent on the binding of the domain to acetyl-CoA, is important for its catalytic activity [69]. For this reason, in the evaluation of small molecules to discover p300 inhibitors, the binding of small molecules to the HAT domain serves as a critical indicator [70,71]. Taken together, our results suggest that PT competitively binds with acetyl-CoA to the p300 HAT domain, which functions as a catalytic pocket, and negatively regulates the transcription of genes by interacting directly with histone tails to obstruct the autoinhibitory function of p300. This indicates a potential application for a new class of PT nutraceuticals with p300 inhibitory activity. Indeed, p300 activity was inhibited with a specific inhibitor, C-646, and genetically by using siRNA against *p300*, both of which were able to effectively reduce the statin-induced increase in *PCSK9* expression. To date, no study has shown that p300 is directly implicated in transcriptionally regulating *PCSK9*; however, several studies have indicated the possibility of epigenetic regulation of PCSK9 expression. In 2013, Dong XC et al. revealed that Sirtuin 6 (Sirt6), an NAD (+)-dependent histone deacetylase, was recruited to the PCSK9 proximal promoter region with the forkhead transcription factor (FOXO3), where it causes deacetylation of histone H3K9 and H3K56 to suppress *PCSK9* and stabilize LDLR expression [27]. Recently, targeting *PCSK9* with three microRNAs (miRNAs), miR-191, miR-222, and miR-224, was shown to decrease its expression in HepG2 cells [72]. These results support our hypothesis that *PCSK9* mRNA expression is epigenetically regulated. Based on these previous reports, to directly confirm the involvement of p300 in *PCSK9* regulation, a ChIP assay was performed with the *PCSK9* promoter region (–339 to –278 bp), which is the site at which p300 is expected to be recruited. Surprisingly, p300 was found to occupy the promoter region following simvastatin treatment, and this interaction was completely obstructed by PT. In general, p300 occupancy correlates with transcriptional activation of a gene [73]. In addition, some reports demonstrated that *HNF1*α, which is responsible for *PCSK9* transcription, forms a coactivator complex with p300/CBP [74,75]. Thus, it is possible that p300 was co-recruited with HNF1α on the *PCSK9* promoter region and enhanced the transcriptional activity of the gene. Furthermore, hyperacetylation on histone tails by p300 facilitates loosening the chromatin structure to thereby accelerate gene transcription [76]. Although we did not fully identify the mechanism of regulation of PCSK9 with statin alone or the statin-PT combination in detail, our study is the first to demonstrate a plausible mechanism by which PT induces statin resistance and tolerance through reducing PCSK9 expression based on an epigenetic mechanism implicating p300.

Finally, our hypothesis was firmly supported by animal experiments designed with minimal modification based on previous studies as mentioned in the Materials and Methods section [36,34,35]. To our knowledge, there have been few attempts to use a phytochemical to alleviate statin side effects in an animal model. As expected, after HFD feeding for 16 weeks, the total-C and LDL-C levels in the blood of mice were significantly reduced in the simvastatin-administered group. These results were consistent with previous studies [34,77]. Interestingly, the simvastatin-PT combination more effectively reduced the LDL-C level compared to simvastatin single treatment in HFD-fed mice. As shown in Fig. 6D, this phenomenon was presumed to be caused by inhibition of the statin-elicited LDLR degradation in the livers of HFD-fed mice following PT administration. However, despite numerous attempts, we unfortunately failed to detect the matured PCSK9 expression in mouse livers. PCSK9 is mainly synthesized, undergoes autocatalytic cleavage (matured form), and is secreted to the blood as a molecular chaperone to direct LDLR degradation [78]. We suspect that the major cause of our failure in this respect was that we overlooked the rapid movement of matured PCKS9 to the blood after its posttranslational modification in the liver.

In summary, the present study demonstrated that PT is a potential p300 inhibitor that represses statin-induced PCSK9 expression and further stabilizes LDLR expression through its p300-inhibitory activity (Fig. 7). This indicates that statin resistance and tolerance could be ameliorated by PT treatment. Although the importance of phytochemicals, including PT, is increasing daily, several issues regarding their practical application remain to be addressed. Moreover, it is necessary to note the limitation of our study. First, although, it is clear that the effects of DLPS-only or the DLPS-statin combination are significantly reduced by PT, the mechanism of action appears to be completely different depending on the cellular environment. We predict that there are complex pharmacological mechanisms beyond our current understanding of this issue. It is therefore important to understand this before proceeding to clinical applications. Second, as mentioned in the preceding paragraph, we failed to detect the expression of the PCSK9 matured form to examine its direct role in LDLR degradation. In addition, we did not measure the PCSK9 level in the blood due to the limited volume available in the present study. Based on the LDLR stabilization and LDL-C reduction following the statin-PT combined treatment compared with those of the statin single treatment group, it could be inferred that statin-induced PCSK9 might be suppressed by PT. Third, we have not been able to directly compare the efficacy of evolocumab with PT owing to lack of availability based on patent issues.

Despite the above limitations, our study strongly suggests a beneficial effect of PT in overcoming statin resistance and tolerance *in vivo*. Furthermore, this study provides the first evidence of the underlying molecular mechanism of these effects from an epigenetic perspective. However, considering the significance of the aforementioned issues, further in-depth studies should be performed to understand the mechanism of action of PT in more detail and the complex network of genes involved to provide a new therapeutic strategy for hypercholesterolemia.

Author contributions

Conceptualization: H.-K.C. and M.-Y.C.; Data curation: J.-T. H.; Funding acquisition: J.-T.H.; Investigation: J.-H.L., H.-J.K., M.-Y. C., S.-W.C., and S.-P.H.; Methodology: J.-H.L., M.-Y.C., S.-H.L., and S.-W.P.; Project administration: H.-K.C. and J.-T.H.; Supervision: H.-K.C. and J.-H.P.; Writing – original draft: H.-K.C., and J.-H.L.; Validation: H.-K.C and J.-H.L.; Writing – review & editing: H.-K.C., and J.-T.H.

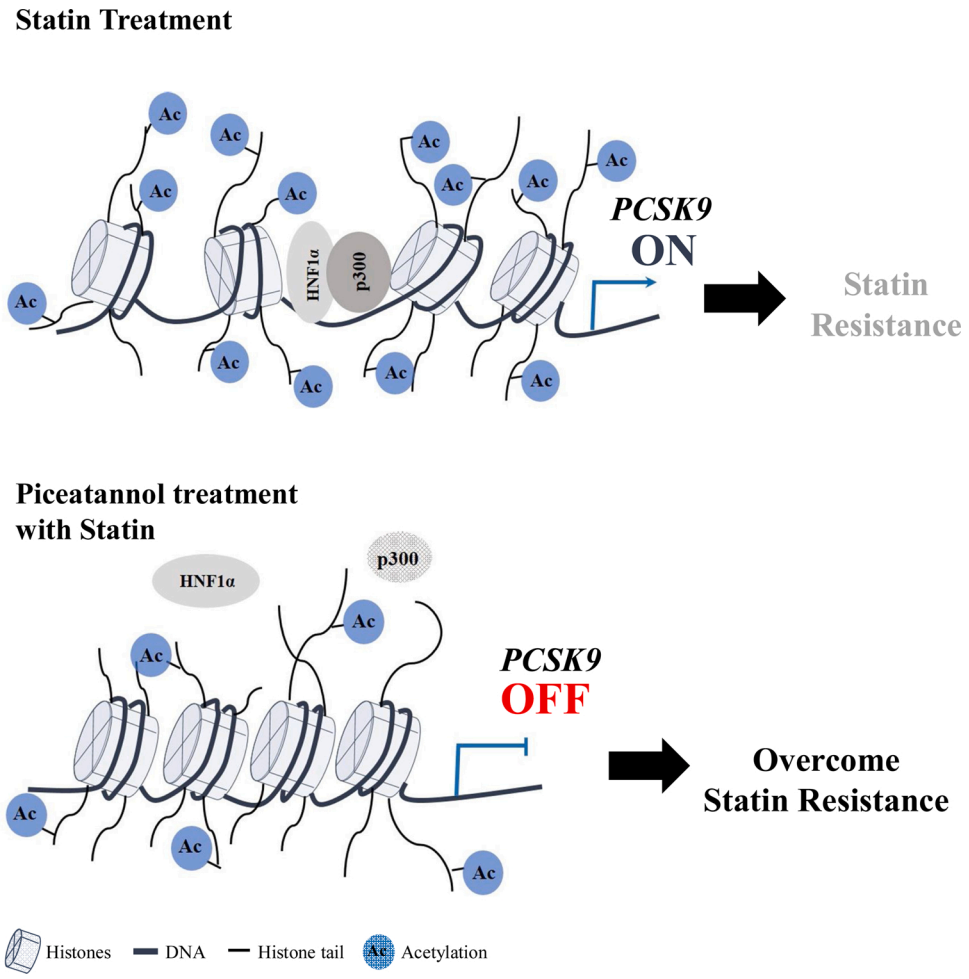

Fig. 7. The potential mechanism of action of PT to ameliorate statin resistance and tolerance. PT reduced statins-triggered excessive PCSK9 expression, resulting in greater stabilization of LDLR, consequently promoting a further decrease of LDL-C in the blood owing to its p300i activity. As a potent HATi, especially p300i, PT can attenuate PCSK9-elicited statin resistance and tolerance. PT abrogates not only the excessive activity of p300 HAT enzyme but also the recruitment p300 to the *PCSK9* promoter region. This consequently inhibits hyperacetylation of the *PCSK9* promoter and maintains the heterochromatin form, thereby reducing the transcriptional activity of the gene. Thus, PT represents a promising candidate dietary compound for ameliorating statin resistance and tolerance caused by excessive PCSK9 expression.

Declaration of Competing Interest

The authors declare that they have no known competing financial interests or personal relationships that could have appeared to influence the work reported in this paper.

Acknowledgements

This work was supported by the Main Research Program (E-0150301) of the Korea Food Research Institute (KFRI), funded by the Ministry of Science, ICT & Future Planning.

Appendix A. Supplementary data

Supplementary material related to this article can be found, in the online version, at doi:https://doi.org/10.1016/j.phrs.2020.105205.

References

[1] E. Ikonen, Cellular cholesterol trafficking and compartmentalization, Nat. Rev. Mol. Cell Biol. 9 (2) (2008) 125–138.
[2] S. Raffy, J. Teissie, Control of lipid membrane stability by cholesterol content, Biophys. J. 76 (4) (1999) 2072–2080.
[3] D. Bhatnagar, H. Soran, P.N. Durrington, Hypercholesterolaemia and its management, BMJ 337 (2008) a993.
[4] G.Y. Chen, L. Li, F. Dai, X.J. Li, X.X. Xu, J.G. Fan, Prevalence of and risk factors for type 2 diabetes mellitus in Hyperlipidemia in China, Med. Sci. Monit. 21 (2015) 2476–2484.
[5] B. Klop, J.W. Elte, M.C. Cabezas, Dyslipidemia in obesity: mechanisms and potential targets, Nutrients 5 (4) (2013) 1218–1240.
[6] R.H. Nelson, Hyperlipidemia as a risk factor for cardiovascular disease, Prim. Care 40 (1) (2013) 195–211.
[7] S.Y. Jiang, H. Li, J.J. Tang, J. Wang, J. Luo, B. Liu, J.K. Wang, X.J. Shi, H.W. Cui, J. Tang, F. Yang, W. Qi, W.W. Qiu, B.L. Song, Discovery of a potent HMG-CoA reductase degrader that eliminates statin-induced reductase accumulation and lowers cholesterol, Nat. Commun. 9 (1) (2018) 5138.
[8] X. Liang, Q. He, Q. Zhao, Effect of stains on LDL reduction and liver safety: a systematic review and meta-analysis, Biomed Res. Int. 2018 (2018), 7092414.
[9] I. Buhaescu, H. Izzedine, Mevalonate pathway: a review of clinical and therapeutical implications, Clin. Biochem. 40 (9–10) (2007) 575–584.
[10] B.A. Golomb, M.A. Evans, Statin adverse effects: a review of the literature and evidence for a mitochondrial mechanism, Am. J. Cardiovasc. Drugs 8 (6) (2008) 373–418.
[11] M.T. Hyyppa, E. Kronholm, A. Virtanen, A. Leino, A. Jula, Does simvastatin affect mood and steroid hormone levels in hypercholesterolemic men? A randomized double-blind trial, Psychoneuroendocrinology 28 (2) (2003) 181–194.
[12] S. Ramkumar, A. Raghunath, S. Raghunath, Statin therapy: review of safety and potential side effects, Acta Cardiol. Sin. 32 (6) (2016) 631–639.
[13] B.A. Taylor, P.D. Thompson, Statins and their effect on PCSK9-Impact and clinical relevance, Curr. Atheroscler. Rep. 18 (8) (2016) 46.
[14] H.J. Kwon, T.A. Lagace, M.C. McNutt, J.D. Horton, J. Deisenhofer, Molecular basis for LDL receptor recognition by PCSK9, Proc. Natl. Acad. Sci. U.S.A. 105 (6) (2008) 1820–1825.
[15] M. Abifadel, M. Varret, J.P. Rabes, D. Allard, K. Ouguerram, M. Devillers, C. Cruaud, S. Benjannet, L. Wickham, D. Erlich, A. Derre, L. Villeger, M. Farnier, I. Beucler, E. Bruckert, J. Chambaz, B. Chanu, J.M. Lecerf, G. Luc, P. Moulin, J. Weissenbach, A. Prat, M. Krempf, C. Junien, N.G. Seidah, C. Boileau, Mutations in PCSK9 cause autosomal dominant hypercholesterolemia, Nat. Genet. 34 (2) (2003) 154–156.
[16] N.G. Seidah, S. Benjannet, L. Wickham, J. Marcinkiewicz, S.B. Jasmin, S. Stifani, A. Basak, A. Prat, M. Chretien, The secretory proprotein convertase neural apoptosis-regulated convertase 1 (NARC-1): liver regeneration and neuronal differentiation, Proc. Natl. Acad. Sci. U.S.A. 100 (3) (2003) 928–933.
[17] M.D. Shapiro, H. Tavori, S. Fazio, PCSK9: from basic science discoveries to clinical trials, Circ. Res. 122 (10) (2018) 1420–1438.
[18] D.W. Zhang, R. Garuti, W.J. Tang, J.C. Cohen, H.H. Hobbs, Structural requirements for PCSK9-mediated degradation of the low-density lipoprotein receptor, Proc. Natl. Acad. Sci. U.S.A. 105 (35) (2008) 13045–13050.

[19] Y. Handelsman, N.E. Lepor, PCSK9 inhibitors in lipid management of patients with diabetes mellitus and high cardiovascular risk: a review, J. Am. Heart Assoc. 7 (13) (2018).
[20] W.C.Y. Binod Pokhrel, Steven N. Levine, PCSK9 Inhibitors, StatPearls, 2020.
[21] A.A. Momtazi, M. Banach, M. Pirro, N. Katsiki, A. Sahebkar, Regulation of PCSK9 by nutraceuticals, Pharmacol. Res. 120 (2017) 157–169.
[22] W. Kong, J. Wei, P. Abidi, M. Lin, S. Inaba, C. Li, Y. Wang, Z. Wang, S. Si, H. Pan, S. Wang, J. Wu, Y. Wang, Z. Li, J. Liu, J.D. Jiang, Berberine is a novel cholesterol-lowering drug working through a unique mechanism distinct from statins, Nat. Med. 10 (12) (2004) 1344–1351.
[23] H. Li, B. Dong, S.W. Park, H.S. Lee, W. Chen, J. Liu, Hepatocyte nuclear factor 1alpha plays a critical role in PCSK9 gene transcription and regulation by the natural hypocholesterolemic compound berberine, J. Biol. Chem. 284 (42) (2009) 28885–28895.
[24] M.H. Tai, P.K. Chen, P.Y. Chen, M.J. Wu, C.T. Ho, J.H. Yen, Curcumin enhances cell-surface LDLR level and promotes LDL uptake through downregulation of PCSK9 gene expression in HepG2 cells, Mol. Nutr. Food Res. 58 (11) (2014) 2133–2145.
[25] M. Maceyka, S. Milstien, S. Spiegel, The potential of histone deacetylase inhibitors in Niemann - pick type C disease, FEBS J. 280 (24) (2013) 6367–6372.
[26] M.J. Nunes, M. Moutinho, I. Milagre, M.J. Gama, E. Rodrigues, Okadaic acid inhibits the trichostatin A-mediated increase of human CYP46A1 neuronal expression in a ERK1/2-Sp3-dependent pathway, J. Lipid Res. 53 (9) (2012) 1910–1919.
[27] R. Tao, X. Xiong, R.A. DePinho, C.X. Deng, X.C. Dong, FoxO3 transcription factor and Sirt6 deacetylase regulate low density lipoprotein (LDL)-cholesterol homeostasis via control of the proprotein convertase subtilisin/kexin type 9 (Pcsk9) gene expression, J. Biol. Chem. 288 (41) (2013) 29252–29259.
[28] Y.L. Tang, S.W. Chan, A review of the pharmacological effects of piceatannol on cardiovascular diseases, Phytother. Res. 28 (11) (2014) 1581–1588.
[29] Y. Setoguchi, Y. Oritani, R. Ito, H. Inagaki, H. Maruki-Uchida, T. Ichiyanagi, T. Ito, Absorption and metabolism of piceatannol in rats, J. Agric. Food Chem. 62 (12) (2014) 2541–2548.
[30] H. Piotrowska, M. Kucinska, M. Murias, Biological activity of piceatannol: leaving the shadow of resveratrol, Mutat. Res. 750 (1) (2012) 60–82.
[31] M.A. Seyed, I. Jantan, S.N. Bukhari, K. Vijayaraghavan, A comprehensive review on the chemotherapeutic potential of piceatannol for Cancer treatment, with mechanistic insights, J. Agric. Food Chem. 64 (4) (2016) 725–737.
[32] Y.J. Surh, H.K. Na, Therapeutic potential and molecular targets of piceatannol in chronic diseases, Adv. Exp. Med. Biol. 928 (2016) 185–211.
[33] V.C. Hannah, J. Ou, A. Luong, J.L. Goldstein, M.S. Brown, Unsaturated fatty acids down-regulate srebp isoforms 1a and 1c by two mechanisms in HEK-293 cells, J. Biol. Chem. 276 (6) (2001) 4365–4372.
[34] X. He, N. Zheng, J. He, C. Liu, J. Feng, W. Jia, H. Li, Gut microbiota modulation attenuated the hypolipidemic effect of simvastatin in high-fat/cholesterol-diet fed mice, J. Proteome Res. 16 (5) (2017) 1900–1910.
[35] R.A. Miller, D.E. Harrison, C. Astle, J.A. Baur, A.R. Boyd, R. De Cabo, E. Fernandez, K. Flurkey, M.A. Javors, J.F. Nelson, Rapamycin, but not resveratrol or simvastatin, extends life span of genetically heterogeneous mice, J. Gerontol. 66 (2) (2011) 191–201.
[36] A. McKay, B.P. Leung, I.B. McInnes, N.C. Thomson, F.Y. Liew, A novel anti-inflammatory role of simvastatin in a murine model of allergic asthma, J. Immunol. 172 (5) (2004) 2903–2908.
[37] S. Kim, J. Chen, T. Cheng, A. Gindulyte, J. He, S. He, Q. Li, B.A. Shoemaker, P. A. Thiessen, B. Yu, L. Zaslavsky, J. Zhang, E.E. Bolton, PubChem 2019 update: improved access to chemical data, Nucleic Acids Res. 47 (D1) (2019) D1102–D1109.
[38] N.M. O'Boyle, M. Banck, C.A. James, C. Morley, T. Vandermeersch, G. R. Hutchison, Open Babel: An open chemical toolbox, J. Cheminform. 3 (2011) 33.
[39] G.M. Morris, R. Huey, W. Lindstrom, M.F. Sanner, R.K. Belew, D.S. Goodsell, A. J. Olson, AutoDock4 and AutoDockTools4: Automated docking with selective receptor flexibility, J. Comput. Chem. 30 (16) (2009) 2785–2791.
[40] O. Trott, A.J. Olson, AutoDock Vina: improving the speed and accuracy of docking with a new scoring function, efficient optimization, and multithreading, J. Comput. Chem. 31 (2) (2010) 455–461.
[41] H.-K. Choi, Y. Choi, E.S. Park, S.-Y. Park, S.-H. Lee, J. Seo, M.-H. Jeong, J.-W. Jeong, J.-H. Cheong, P.C. Lee, Programmed cell death 5 mediates HDAC3 decay to promote genotoxic stress response, Nat. Commn. 6 (1) (2015) 1–18.
[42] H. Tavori, D. Fan, J.L. Blakemore, P.G. Yancey, L. Ding, M.F. Linton, S. Fazio, Serum proprotein convertase subtilisin/kexin type 9 and cell surface low-density lipoprotein receptor: evidence for a reciprocal regulation, Circulation 127 (24) (2013) 2403–2413.
[43] J. Zhou, C. Zhu, H. Luo, L. Shen, J. Gong, Y. Wu, J. Magdalou, L. Chen, Y. Guo, H. Wang, Two intrauterine programming mechanisms of adult hypercholesterolemia induced by prenatal nicotine exposure in male offspring rats, FASEB J. 33 (1) (2019) 1110–1123.
[44] G.D. Bowman, M.G. Poirier, Post-translational modifications of histones that influence nucleosome dynamics, Chem. Rev. 115 (6) (2015) 2274–2295.
[45] H.J. Avis, M.N. Vissers, E.A. Stein, F.A. Wijburg, M.D. Trip, J.J. Kastelein, B. A. Hutten, A systematic review and meta-analysis of statin therapy in children with familial hypercholesterolemia, Arterioscler. Thromb. Vasc. Biol. 27 (8) (2007) 1803–1810.
[46] D. Marks, M. Thorogood, H.A. Neil, S.E. Humphries, A review on the diagnosis, natural history, and treatment of familial hypercholesterolaemia, Atherosclerosis 168 (1) (2003) 1–14.
[47] L.G. Vladimirova-Kitova, S.I. Kitov, Resistance of statin therapy, and methods for its influence, Hypercholesterolemia (2015) 185.
[48] S. Rashid, D.E. Curtis, R. Garuti, N.N. Anderson, Y. Bashmakov, Y. Ho, R. E. Hammer, Y.-A. Moon, J.D. Horton, Decreased plasma cholesterol and hypersensitivity to statins in mice lacking Pcsk9, Proc. Natl. Acad. Sci. U.S.A. 102 (15) (2005) 5374–5379.
[49] M.P. Zimmerman, How do PCSK9 inhibitors stack up to statins for low-density lipoprotein cholesterol control, Am. Health Drug Benefits 8 (8) (2015) 436–442.
[50] H.J. Lee, M.G. Kang, H.Y. Cha, Y.M. Kim, Y. Lim, S.J. Yang, Effects of piceatannol and resveratrol on sirtuins and hepatic inflammation in high-fat diet-fed mice, J. Med. Food 22 (8) (2019) 833–840.
[51] Y.C. Tung, Y.H. Lin, H.J. Chen, S.C. Chou, A.C. Cheng, N. Kalyanam, C.T. Ho, M. H. Pan, Piceatannol exerts anti-obesity effects in C57BL/6 mice through modulating adipogenic proteins and gut microbiota, Molecules 21 (11) (2016).
[52] M. Minakawa, Y. Miura, K. Yagasaki, Piceatannol, a resveratrol derivative, promotes glucose uptake through glucose transporter 4 translocation to plasma membrane in L6 myocytes and suppresses blood glucose levels in type 2 diabetic model db/db mice, Biochem. Biophys. Res. Commun. 422 (3) (2012) 469–475.
[53] H. Uchida-Maruki, H. Inagaki, R. Ito, I. Kurita, M. Sai, T. Ito, Piceatannol lowers the blood glucose level in diabetic mice, Biol. Pharm. Bull. 38 (4) (2015) 629–633.
[54] B. Dong, M. Wu, H. Li, F.B. Kraemer, K. Adeli, N.G. Seidah, S.W. Park, J. Liu, Strong induction of PCSK9 gene expression through HNF1alpha and SREBP2: mechanism for the resistance to LDL-cholesterol lowering effect of statins in dyslipidemic hamsters, J. Lipid Res. 51 (6) (2010) 1486–1495.
[55] V.R. Shende, M. Wu, A.B. Singh, B. Dong, C.F. Kan, J. Liu, Reduction of circulating PCSK9 and LDL-C levels by liver-specific knockdown of HNF1alpha in normolipidemic mice, J. Lipid Res. 56 (4) (2015) 801–809.
[56] S. Rong, V.A. Cortes, S. Rashid, N.N. Anderson, J.G. McDonald, G. Liang, Y. A. Moon, R.E. Hammer, J.D. Horton, Expression of SREBP-1c requires SREBP-2-mediated generation of a sterol ligand for LXR in livers of mice, Elife 6 (2017).
[57] A. Ochiai, S. Miyata, M. Shimizu, J. Inoue, R. Sato, Piperine induces hepatic low-density lipoprotein receptor expression through proteolytic activation of sterol regulatory element-binding proteins, PLoS One 10 (10) (2015), e0139799.
[58] Y. Zhang, K.L. Ma, X.Z. Ruan, B.C. Liu, Dysregulation of the low-density lipoprotein receptor pathway is involved in lipid disorder-mediated organ injury, Int. J. Biol. Sci. 12 (5) (2016) 569–579.
[59] V. Sorrentino, N. Zelcer, Post-transcriptional regulation of lipoprotein receptors by the E3-ubiquitin ligase inducible degrader of the low-density lipoprotein receptor, Curr. Opin. Lipidol. 23 (3) (2012) 213–219.
[60] E. Scotti, C. Hong, Y. Yoshinaga, Y. Tu, Y. Hu, N. Zelcer, R. Boyadjian, P.J. de Jong, S.G. Young, L.G. Fong, P. Tontonoz, Targeted disruption of the idol gene alters cellular regulation of the low-density lipoprotein receptor by sterols and liver x receptor agonists, Mol. Cell. Biol. 31 (9) (2011) 1885–1893.
[61] A. Peserico, C. Simone, Physical and functional HAT/HDAC interplay regulates protein acetylation balance, J. Biomed. Biotechnol. 2011 (2011), 371832.
[62] K.C. Choi, M.G. Jung, Y.H. Lee, J.C. Yoon, S.H. Kwon, H.B. Kang, M.J. Kim, J. H. Cha, Y.J. Kim, W.J. Jun, J.M. Lee, H.G. Yoon, Epigallocatechin-3-gallate, a histone acetyltransferase inhibitor, inhibits EBV-induced B lymphocyte transformation via suppression of RelA acetylation, Cancer Res. 69 (2) (2009) 583–592.
[63] M. Ghizzoni, J. Wu, T. Gao, H.J. Haisma, F.J. Dekker, Y. George Zheng, 6-alkylsalicylates are selective Tip60 inhibitors and target the acetyl-CoA binding site, Eur. J. Med. Chem. 47 (1) (2012) 337–344.
[64] M.G. Marcu, Y.J. Jung, S. Lee, E.J. Chung, M.J. Lee, J. Trepel, L. Neckers, Curcumin is an inhibitor of p300 histone acetylatransferase, Med. Chem. 2 (2) (2006) 169–174.
[65] M.Y. Chung, J.H. Song, J. Lee, E.J. Shin, J.H. Park, S.H. Lee, J.T. Hwang, H.K. Choi, Tannic acid, a novel histone acetyltransferase inhibitor, prevents non-alcoholic fatty liver disease both in vivo and in vitro model, Mol. Metab. 19 (2019) 34–48.
[66] M.A. Islam, F. Alam, M. Solayman, M.I. Khalil, M.A. Kamal, S.H. Gan, Dietary phytochemicals: natural swords combating inflammation and oxidation-mediated degenerative diseases, Oxid. Med. Cell. Longev. 2016 (2016), 5137431.
[67] H. Wapenaar, F.J. Dekker, Histone acetyltransferases: challenges in targeting bi-substrate enzymes, Clin. Epigenetics 8 (2016) 59.
[68] C.W. Hsu, D. Shou, R. Huang, T. Khuc, S. Dai, W. Zheng, C. Klumpp-Thomas, M. Xia, Identification of HDAC inhibitors using a cell-based HDAC I/II assay, J. Biomol. Screen. 21 (6) (2016) 643–652.
[69] P.R. Thompson, D. Wang, L. Wang, M. Fulco, N. Pediconi, D. Zhang, W. An, Q. Ge, R.G. Roeder, J. Wong, M. Levrero, V. Sartorelli, R.J. Cotter, P.A. Cole, Regulation of the p300 HAT domain via a novel activation loop, Nat. Struct. Mol. Biol. 11 (4) (2004) 308–315.
[70] B. Karanam, L. Jiang, L. Wang, N.L. Kelleher, P.A. Cole, Kinetic and mass spectrometric analysis of p300 histone acetyltransferase domain autoacetylation, J. Biol. Chem. 281 (52) (2006) 40292–40301.
[71] J. Maksimoska, D. Segura-Pena, P.A. Cole, R. Marmorstein, Structure of the p300 histone acetyltransferase bound to acetyl-coenzyme A and its analogues, Biochemistry 53 (21) (2014) 3415–3422.
[72] P. Naeli, F. Mirzadeh Azad, M. Malakootian, N.G. Seidah, S.J. Mowla, Post-transcriptional regulation of PCSK9 by miR-191, miR-222, and miR-224, Front. Genet. 8 (2017) 189.
[73] L.H. Kasper, S. Lerach, J. Wang, S. Wu, T. Jeevan, P.K. Brindle, CBP/p300 double null cells reveal effect of coactivator level and diversity on CREB transactivation, EMBO J. 29 (21) (2010) 3660–3672.
[74] N. Ban, Y. Yamada, Y. Someya, K. Miyawaki, Y. Ihara, M. Hosokawa, S. Toyokuni, K. Tsuda, Y. Seino, Hepatocyte nuclear factor-1α recruits the transcriptional co-activator p300 on the GLUT2 gene promoter, Diabetes 51 (5) (2002) 1409–1418.

[75] E. Soutoglou, G. Papafotiou, N. Katrakili, I. Talianidis, Transcriptional activation by hepatocyte nuclear factor-1 requires synergism between multiple coactivator proteins, J. Biol. Chem. 275 (17) (2000) 12515–12520.
[76] A. Goel, R. Janknecht, Acetylation-mediated transcriptional activation of the ETS protein ER81 by p300, P/CAF, and HER2/Neu, Mol. Cell. Biol. 23 (17) (2003) 6243–6254.
[77] J.-W. Chen, Y.-L. Lin, C.-H. Chou, Y.-H.S. Wu, S.-Y. Wang, Y.-C. Chen, Antiobesity and hypolipidemic effects of protease A-digested crude-chalaza hydrolysates in a high-fat diet, J. Funct. Foods 66 (2020), 103788.
[78] A. Grefhorst, M.C. McNutt, T.A. Lagace, J.D. Horton, Plasma PCSK9 preferentially reduces liver LDL receptors in mice, J. Lipid Res. 49 (6) (2008) 1303–1311.